Cancer Cell
Article

Integrative Genomics Analysis Reveals Silencing of β-Adrenergic Signaling by Polycomb in Prostate Cancer

Jindan Yu,[1] Qi Cao,[1,8] Rohit Mehra,[1,8] Bharathi Laxman,[1] Jianjun Yu,[1,5] Scott A. Tomlins,[1] Chad J. Creighton,[5] Saravana M. Dhanasekaran,[1] Ronglai Shen,[3] Guoan Chen,[6] David S. Morris,[2] Victor E. Marquez,[7] Rajal B. Shah,[1,2] Debashis Ghosh,[3] Sooryanarayana Varambally,[1,4] and Arul M. Chinnaiyan[1,2,4,5,*]
[1]Department of Pathology, Michigan Center for Translational Pathology
[2]Department of Urology
[3]Department of Biostatistics
[4]Comprehensive Cancer Center
[5]Bioinformatics Program
[6]Department of Surgery
University of Michigan Medical School, Ann Arbor, MI 48109, USA
[7]Laboratory of Medical Chemistry, Center for Cancer Research, National Cancer Institute-Frederick, National Institute of Health, Frederick, MD 21702, USA
[8]These authors contributed equally to this work.
*Correspondence: arul@umich.edu
DOI 10.1016/j.ccr.2007.10.016

SUMMARY

The Polycomb group (PcG) protein EZH2 possesses oncogenic properties for which the underlying mechanism is unclear. We integrated in vitro cell line, in vivo tumor profiling, and genome-wide location data to nominate key targets of EZH2. One of the candidates identified was *ADRB2* (Adrenergic Receptor, Beta-2), a critical mediator of β-adrenergic signaling. EZH2 is recruited to the *ADRB2* promoter and represses ADRB2 expression. ADRB2 inhibition confers cell invasion and transforms benign prostate epithelial cells, whereas ADRB2 overexpression counteracts EZH2-mediated oncogenesis. ADRB2 is underexpressed in metastatic prostate cancer, and clinically localized tumors that express lower levels of ADRB2 exhibit a poor prognosis. Taken together, we demonstrate the power of integrating multiple diverse genomic data to decipher targets of disease-related genes.

INTRODUCTION

The Polycomb group (PcG) proteins are transcriptional repressors important for preserving cellular identity (Ringrose and Paro, 2004) and maintaining pluripotency and plasticity of embryonic stem cells (Boyer et al., 2006; Lee et al., 2006). They function in multiprotein Polycomb Repressive Complexes (PRCs), one of which is PRC2 (Levine et al., 2002). PRC2 includes SUZ12 (Suppressor of Zeste 12), EED (Embryonic Ectoderm Development), and EZH2 (Enhancer of Zeste 2) and is essential for the initial binding to target gene promoters (Rastelli et al., 1993). EZH2 is a histone methyltransferase (HMTase) that specifically methylates lysine 27 of histone H3 (H3K27), thus leading to target gene silencing (Cao et al., 2002; Kirmizis et al., 2004; Kuzmichev et al., 2002).

Dysregulation of EZH2 has recently been associated with a number of cancers, including melanoma, lymphoma, and breast and prostate cancers (Bracken et al., 2003; Varambally et al., 2002; Visser et al., 2001). EZH2 is a

SIGNIFICANCE

The transcriptional corepressor EZH2 possesses oncogenic properties, perhaps through repressing critical tumor suppressor genes. Here we integrated multiple diverse genomic data to nominate direct targets of EZH2. We found that the EZH2-containing Polycomb Repressive Complexes 2 (PRC2) bind to the *ADRB2* promoter and repress ADRB2 expression. Importantly, ADRB2 inhibition induces cell invasiveness and transforms benign prostate epithelial cells. ADRB2 activation in xenograft mouse models inhibits prostate cancer tumor growth in vivo. Remarkably, tissue microarray analysis suggests that ADRB2 may serve as a biomarker of prostate cancer aggressiveness. Therefore, the identification of ADRB2 as a direct target of EZH2 may have implications in prostate cancer prognosis and therapeutic intervention.

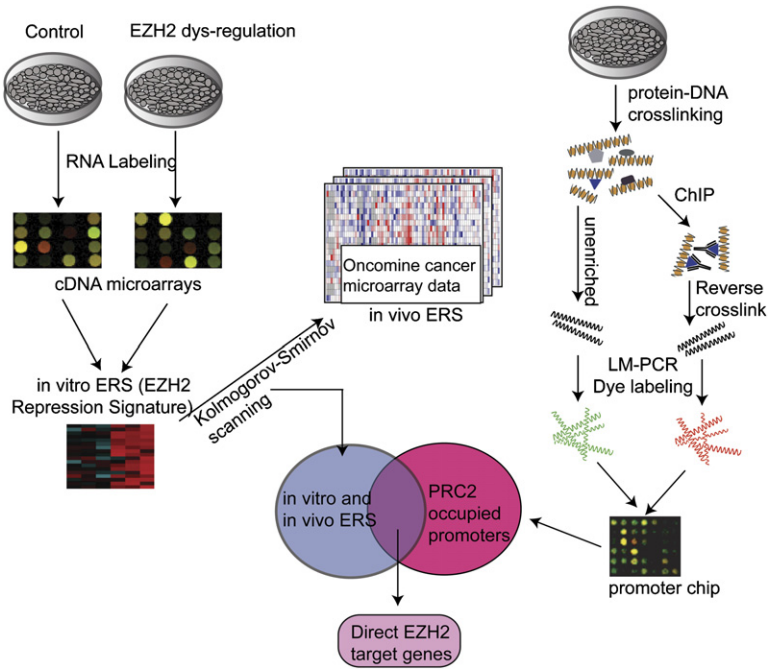

Figure 1. Overview of the Integrative Genomics Analysis used to Nominate Direct EZH2 Transcriptional Targets with Pathological Relevance

Transcriptional targets of EZH2 repression in vitro were identified by expression profiling of immortalized RWPE benign prostate epithelial cells and H16N2 normal breast epithelial cells treated with either EZH2 adenovirus or EZH2 siRNA as described in the Supplemental Experimental Procedures. This in vitro EZH2 repression signature (ERS) was evaluated for its inverse association with EZH2 in vivo by Kolmogorov-Smirnov (KS) (Lamb et al., 2003) scanning of multiple microarray data sets of human tumors in the Oncomine database (Rhodes et al., 2004) (see Figure S1 for significance of association). In vivo ERS was created by selecting genes that showed the most significant repression by EZH2 in vivo. In parallel, a cohort of gene promoters occupied by the PRC2 complex was identified by genome-wide location analysis (Figure S2). The in vivo ERS genes that are also physically bound by the PRC2 complex were nominated as direct EZH2 targets in cancer.

biomarker of aggressive epithelial tumors, and its upregulation correlates with poor prognosis (Bachmann et al., 2006; Collett et al., 2006; Matsukawa et al., 2006; Raaphorst et al., 2003). Functional studies have demonstrated that *EZH2* is a bona fide oncogene. For example, EZH2 RNA interference results in growth arrest in multiple myeloma cells (Croonquist and Van Ness, 2005) as well as in the TIG3 diploid human fibroblasts (Bracken et al., 2003), whereas ectopic overexpression of EZH2 promotes cell proliferation and invasion in vitro (Bracken et al., 2003; Kleer et al., 2003; Varambally et al., 2002) and induces xenograft tumor growth in vivo (Croonquist and Van Ness, 2005). However, the underlying mechanism of EZH2-mediated oncogenesis remains unclear. In this study we hypothesized that EZH2 induces tumorigenesis via direct transcriptional repression of key tumor suppressor genes. We integrated genome-wide expression and location data to identify direct EZH2 targets in cancer. One of the most promising target genes we identified was *ADRB2* (Adrenergic Receptor, Beta-2).

ADRB2 is a G protein-Coupled Receptor (GPCR) of the β-adrenergic signaling pathway. Polymorphisms of the *ADRB2* gene have been associated with increased risk of breast and colorectal cancer (Takezaki et al., 2001). Stimulation of ADRB2 elevates the intracellular level of cyclic AMP (cAMP), which in turn controls a wide range of cellular processes via multiple mechanisms. In particular, activation of cAMP-Rap1 by ADRB2 has been shown to regulate cell adhesion and cellular transformation (Price et al., 2004). However, the role of ADRB2 in prostate cancer progression, especially in the context of Polycomb regulation, has not been investigated. In this study, we demonstrate that ADRB2 is a direct target of EZH2 and establish a role for β-adrenergic signaling in prostate cancer progression.

RESULTS

Identification of ADRB2 as a Direct Target of EZH2 in Prostate Cancer

The purpose of this study is to characterize key direct targets of EZH2 that may confer its oncogenic properties. As EZH2 may regulate a large number of downstream molecules, we integrated multiple diverse genomic data and applied a number of inclusion criteria for target gene selection, thus minimizing the false-positive rates (Figure 1). To investigate gene expression regulated by EZH2 dysregulation, we profiled benign immortalized RWPE prostate and H16N2 breast cell lines using 20k-element cDNA microarrays. As described in the Supplemental Data available with this article online, we identified 139 features (representing 126 unique genes), defined as an "in vitro EZH2 Repression Signature (ERS)," that are repressed by EZH2 adenovirus overexpression compared to control adenovirus-treated cells, as well as upregulated (derepressed) by EZH2 RNA interference relative to control siRNA-treated cells (Table S1). As EZH2 plays a critical role in human cancer progression, we were most interested in EZH2-regulated genes with clinical relevance. To look for a subset of the in vitro ERS genes with coordinate repression by EZH2 in vivo, we interrogated several public gene expression data sets of human tumors from Oncomine (Rhodes et al., 2004), including two prostate (Glinsky et al., 2004; Yu et al., 2004) and two breast cancer data sets (Huang et al., 2003; van 't Veer et al., 2002), and the Global Cancer Map data set consisting of 190 primary human tumors (Ramaswamy et al., 2001). We selected these cancer profiling data sets, as EZH2 is best characterized in prostate and breast cancer. The expression pattern of the in vitro ERS genes as a group showed marked inverse association

with *EZH2* transcript levels in all data sets (Figure S1). Out of these, 23 individual genes were significantly downregulated ($p < 0.05$ by Student's t test) in tumors with higher levels of EZH2 and thus selected as an "in vivo ERS" for further investigation. Notably, a large number of these genes have been previously implicated in cell proliferation and cell adhesion.

EZH2 is a transcriptional repressor that may regulate downstream gene expression either through direct transcriptional regulation or by subsequent effects. To determine primary targets of EZH2, we mapped the genome-wide location of the PRC2 complex using antibodies against SUZ12, which has been successfully studied for large-scale promoter occupancy (Boyer et al., 2006; Bracken et al., 2006; Kirmizis et al., 2004; Lee et al., 2006). We examined two prostate cancer cell lines, PC3 and LNCaP, to increase the robustness of target genes. As described in the Supplemental Data, we identified 85 PRC2-occupied genes in PC3 cells and 78 in LNCaP. Out of these, we observed a remarkable overlap of 63 genes, suggesting the accuracy of this assay (Table S2). In addition, we validated a randomly selected set of three putative targets (NAT1, TUBB, and ZIC1) by conventional chromatin immunoprecipitation (ChIP) followed by PCR (ChIP-PCR) assay (Figure S2).

We compiled gene expression and promoter binding data in order to identify direct EZH2 targets in prostate cancer. Out of the 23 in vivo ERS genes identified from our transcriptome analysis, two genes, namely *ADRB2* and *IGFBP2*, are directly occupied by PRC2. In this study we characterized the role of ADRB2 in the context of EZH2 oncogenic function in prostate cancer, as ADRB2 has been previously implicated to have a role in cell growth, adhesion, and transformation (Bos, 2005).

EZH2 Represses Transcript and Protein Levels of ADRB2

To confirm that EZH2 represses ADRB2, we experimentally overexpressed EZH2 by adenoviral infection of multiple benign prostate and breast cell lines. Quantitative RT-PCR demonstrated significantly reduced levels of *ADRB2* transcript in response to EZH2 overexpression relative to adenoviral vector control cells (Figure 2A and Figure S3). This downregulation of ADRB2 was not observed with the overexpression of an EZH2 mutant (EZH2ΔSET) lacking the SET domain that is responsible for the HMTase activity of EZH2. To determine whether ADRB2 protein is coordinately regulated, we performed immunoblot analysis of ADRB2 and observed a major band of predicted size (47 kDa), supporting the specificity of the antibody (Figure S3). Consistent with the changes at the transcript level, EZH2 overexpression markedly reduced the expression of ADRB2 protein when compared to the vector and EZH2ΔSET controls (Figure 2B). Additionally, to localize ADRB2 and EZH2 proteins in cells, we performed confocal immunofluorescent staining in the H16N2 primary breast cell lines following vector or EZH2 adenoviral infection. As expected, we found ADRB2 staining primarily in the cell membrane/cytoplasm but EZH2 protein in the cell nucleus (Figure 2C). Notably, in cells infected with EZH2 adenovirus, thus exhibiting strong EZH2 nuclear staining, we observed a marked reduction in ADRB2 staining. By contrast, the vector-infected cells demonstrated absent/low EZH2 and high ADRB2 expression.

We have observed that ADRB2 is in general expressed at lower levels in prostate cancer cells compared to benign prostate epithelial cells, being opposite or inverse to EZH2 expression (data not shown). We hypothesized that this low level of ADRB2 in prostate cancer cells may be due to its repression by high EZH2. To test this hypothesis we examined whether EZH RNA interference can derepress ADRB2 expression in cell line models. Immunoblot analysis demonstrated upregulated ADRB2 protein levels in response to transient EZH2 knockdown (Figure 2D). This upregulation is more prominent in LNCaP and PC3 prostate cancer cells (over 2-fold) than in primary cell lines (less than 2-fold). As transient RNA interference of EZH2 only moderately induces ADRB2, we attempted to establish DU145-shEZH2 cell lines with long-term inhibition of EZH2 using short-hairpin RNAs (shRNAs) followed by selection of stable colonies. Stable inhibition of EZH2 led to a marked increase of ADRB2 protein level (Figure 2E). Importantly, we observed a strong negative association ($r = -0.98$, $p = 0.004$) between EZH2 and ADRB2 protein levels in stable DU145-shEZH2 colonies with varying degrees of EZH2 inhibition, thus providing compelling evidence for EZH2-mediated repression of ADRB2. To assure that EZH2 regulation of ADRB2 occurs at the transcript level, we examined *ADRB2* and *EZH2* transcripts by qRT-PCR. We demonstrated that transient EZH2 RNA interference upregulates *ADRB2* mRNA in both the MDA-MB-231 breast and the DU145 prostate cancer cell lines (Figure 2F).

We next examined whether this regulation has functional relevance in vivo in human tumors. We hypothesized that ADRB2 and EZH2 expression are negatively associated in human prostate tumors. To confirm this, we analyzed their expression in a set of three benign prostate tissue samples, five clinically localized prostate cancers, and seven metastatic prostate cancers by qRT-PCR. As expected, our results demonstrated significant overexpression of *EZH2* ($p < 0.001$ by Wilcoxon rank-sum test), and yet marked downregulation of *ADRB2* ($p < 0.001$ by Wilcoxon rank-sum test) in metastatic prostate cancer compared to organ-confined disease (Figure 2G). Remarkably, the expression levels of *EZH2* and *ADRB2* displayed a strong negative association ($r = -0.67$, $p < 0.001$) across all samples, consistent with the repression of *ADRB2* by *EZH2*.

The EZH2-Containing PRC2 Complex Occupies the *ADRB2* Promoter

Expression regulation of target genes by a transcription factor or cofactors may be mediated through direct interaction or secondary effects. Our genome-wide location analysis suggested that the *ADRB2* promoter may be directly occupied by the PRC2 complex protein SUZ12 in LNCaP and PC3 prostate cancer cells. We thus attempted to recapitulate this protein-promoter binding in multiple

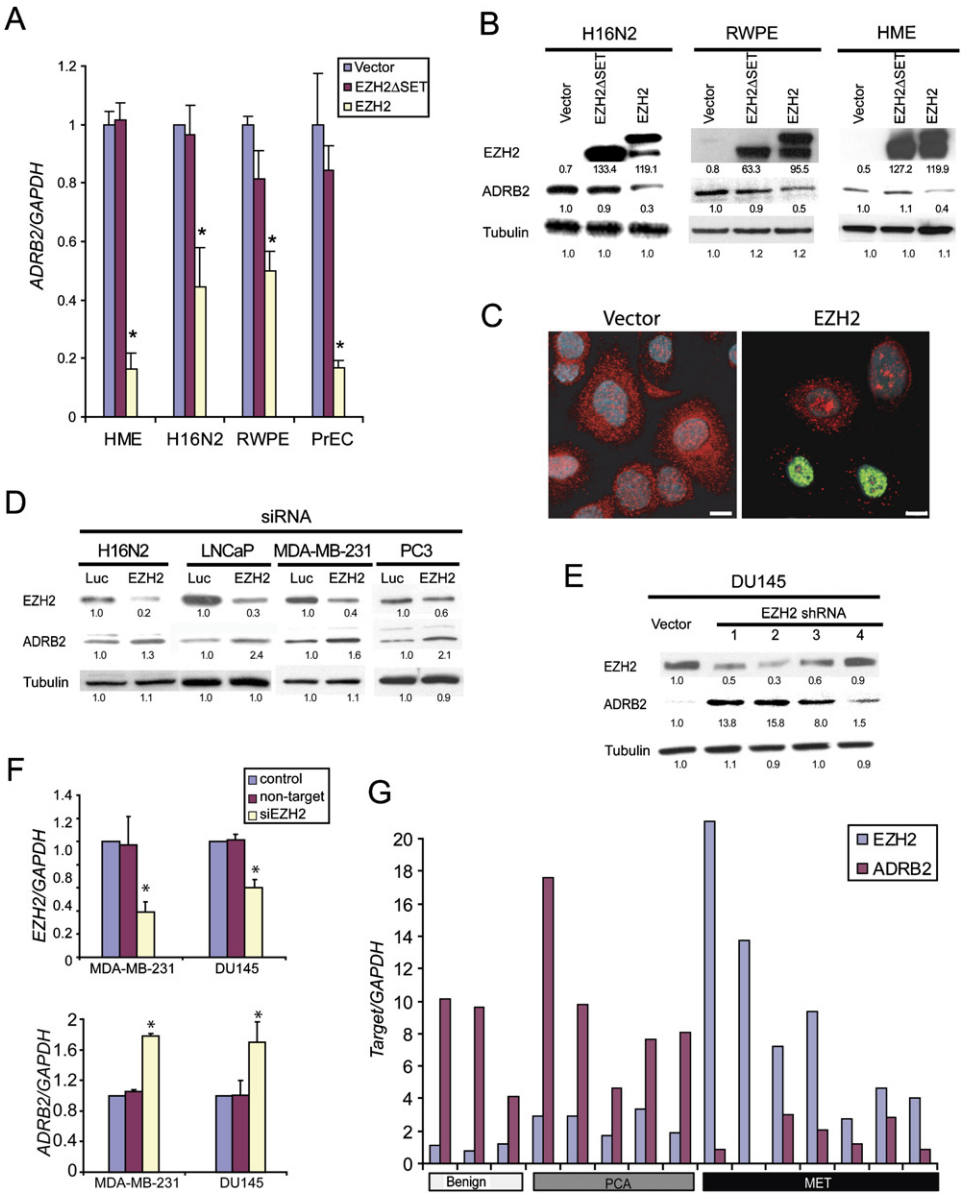

Figure 2. EZH2 Dysregulation Negatively Regulates ADRB2 Transcript and Protein

(A and B) Quantitative RT-PCR analysis for the expression of *ADRB2* transcript (A) and immunoblot analysis of EZH2, ADRB2, and β-tubulin protein (B) in immortalized primary human mammary epithelial cells (HME and H16N2) and prostate epithelial cells (RWPE and PrEC) following infection with vector adenovirus (vector) or adenovirus encoding EZH2 or EZH2ΔSET mutant for 48 hr. See Figure S3 for an assessment of EZH2 transcript level, a complete blot of ADRB2, and a higher exposure of EZH2 immunoblot. In immunoblots, the number underneath each band indicates the intensity of corresponding band. Significant changes in EZH2 samples were evaluated relative to vector control.

(C) Immunofluorescence costaining of ADRB2 (red) and EZH2 (green) in H16N2 cells following adenoviral infection of control vector or EZH2 for 48 hr. Scale bar, 10 μm.

(D) Immunoblot analysis of EZH2 and ADRB2 expression in multiple cell lines following RNA interference of EZH2 or a control. The protein levels of β-tubulin are used as a loading control.

(E) Immunoblot analysis of EZH2 and ADRB2 in four stable DU145-shEZH2 colonies. DU145 cells were transfected with shRNA constructs targeting EZH2 or a vector control, and selected for stable colonies. Individual DU145-shEZH2 colonies varied at the degree of EZH2 inhibition were selected for assessment of the association between the expression levels of EZH2 and ADRB2.

(F) QRT-PCR analysis of *EZH2* and *ADRB2* transcripts in MDA-MB-231 and DU145 cancer cell lines following RNA interference of EZH2 or controls.

(G) QRT-PCR assessment of *EZH2* and *ADRB2* expression in prostate tumor specimens. Expression was determined in a cohort of three benign prostate hyperplasia (benign), five localized prostate cancer (PCA), and seven metastatic prostate cancer (MET) tissues. For QRT-PCR experiments, expression of target genes was normalized to the amount of the housekeeping gene GAPDH.

Error bars: n = 3, mean ± SEM, *p < 0.01 by Student's t test.

cancer cell lines as well as in metastatic prostate tumors. We first examined the LNCaP cells by ChIP using antibodies against EZH2, SUZ12, the EZH2-mediated H3K27 trimethylation (3mH3K27), and an IgG antibody control. By conventional ChIP-PCR assay using primers specific to the *ADRB2* promoter, we observed a strong enrichment (over 30-fold, $p < 0.001$) by EZH2, SUZ12, and 3mH3K27 antibodies relative to the IgG control (Figure 3A).

It is important to investigate whether PRC2 binding on the *ADRB2* promoter is a robust phenomenon across multiple cell lines in vitro and prostate cancer tissues in vivo. Thus, we performed ChIP analysis in a panel of additional samples including the PC3 prostate cancer cell line and 293 human embryonic kidney cell line, as well as three independent metastatic prostate cancer tissues. To provide controls for comparison we analyzed a previously reported PRC2 target gene *CNR1* (Kirmizis et al., 2004) as a positive control and ACTIN as a negative control. Considering the limited amount of tissues available, ChIP-enriched chromatin was amplified along with the whole-cell extract (WCE) DNA to generate enough material for testing multiple target genes. Using an equal amount of amplified WCE and ChIP-enriched DNA, PCR analysis of target genes were evaluated for ChIP enrichment relative to WCE. Our results showed that the PRC2 complex and the 3mH3K27 mark co-occupy the promoters of *ADRB2* and *CNR1*, but not of *ACTIN*, in both PC3 (Figure 3B) and 293 cells (Figure 3C). The 3mH3K27 mark was found to occupy the *ADRB2* promoter in all three metastatic prostate cancer tissues, supporting repression of ADRB2 in vivo (Figure 3D).

We next determined whether EZH2 expression is crucial for PRC2 binding and H3K27 trimethylation of the *ADRB2* promoter. By combining ChIP-PCR assay with RNA interference in the EZH2-high LNCaP prostate cancer cell, we found that siRNA inhibition of EZH2 greatly decreased its occupancy and, importantly, also reduced H3K27 trimethylation of the *ADRB2* promoter and a positive control (Figure 3E). Similarly, we examined the effect of EZH2 overexpression on PRC2 recruitment to the *ADRB2* promoter in the H16N2 primary breast cell line that expresses low levels of endogenous EZH2. We used an antibody against the Myc-tag of the EZH2 adenoviral constructs for ChIP in order to precisely monitor the binding effects of ectopic EZH2. Our results demonstrated the recruitment of Myc-EZH2 to the *ADRB2* promoter, but not of the vector and the EZH2ΔSET mutant, this binding being sensitive to SAHA, which inhibits HDAC activity and blocks histone deacetylation (Figure 3F). Interestingly, ChIP showed markedly increased occupancy of the PRC2 complex proteins EED and SUZ12, as well as 3mH3K27 on the *ADRB2* promoter, upon EZH2 overexpression relative to vector control, whereas the binding of acetylated H3 was strongly reduced, indicative of increased histone deacetylation (Figure 3G). Further evaluation of SAHA revealed a marked reduction of PRC2 binding and consequent H3K27 trimethylation, and accumulation of acetylated H3 at the *ADRB2* promoter (Figures 3H and 3I). QRT-PCR analysis showed corresponding upregulation of *ADRB2* transcripts following a time course of SAHA treatment (Figure 3J).

Tan et al. have recently identified a small-molecule compound, DZNep, which effectively inhibits the expression of PRC2 complex proteins (Tan et al., 2007). To further confirm that ADRB2 is a transcriptional target of PRC2 we examined the effect of DZNep across a batch of breast and prostate cancer cell lines. Our results demonstrated strong induction (derepression) of *ADRB2* in all cell lines tested (Figure 3K).

ADRB2 Inhibition Confers Cell Invasion and Transforms Benign Prostate Epithelial Cells

We have shown above that ADRB2 is a direct target of EZH2 transcriptional repression and is downregulated in metastatic prostate cancer. Thus, we recapitulated this event in benign prostatic epithelial cells to determine the role of aberrant ADRB2 inhibition in prostate cancer. We transfected the immortalized benign prostate epithelial cell line RWPE with shRNA constructs targeting ADRB2 and selected for stable RWPE cells with ADRB2 knockdown (RWPE-shADRB2) cells. The stable RWPE-shADRB2 cells showed a marked reduction in ADRB2 expression relative to the vector-transfected control cells (Figure 4A). We then investigated the effect of ADRB2 inhibition on various oncogenic properties, such as cell proliferation, invasion, and migration. Our results demonstrate that inhibition of ADRB2 had no significant effect on cell proliferation (Figure S4). However, we observed over 5-fold increase of invasion in RWPE-shADRB2 cells compared to the vector control (Figures 4A and 4B). Similarly, inactivation of ADRB2 by the ADRB2-specific antagonist ICI 118,551 significantly increased invasion in RWPE cells (Figure 4C). Concordant with this, cell migration assay by scratch wound healing showed that the RWPE-shADRB2 cells have markedly increased motility than the vector control cells (Figure S5). Taken together, these results suggest that inhibition of ADRB2 in benign prostate cells confers increased invasion, an important oncogenic phenotype.

To confirm the effect of ADRB2 on cell invasion in additional models, we activated ADRB2 using the agonist isoproterenol in DU145 prostate cancer cells and the invasive RWPE-shADRB2 stable cells. The agonist-activated cells showed significantly reduced invasion in both cell lines (Figure S6). Concordantly, invasion assays revealed significantly reduced invasion of the DU145-shEZH2 cells with stable EZH2 knockdown and ADRB2 induction.

To directly link ADRB2 expression with oncogenic EZH2 function, we investigated whether ADRB2 interferes with EZH2-mediated cell invasion. We have previously reported that overexpression of EZH2 increases invasion in immortalized mammary epithelial cell line H16N2 (Kleer et al., 2003). We investigated whether ADRB2 overexpression is able to rescue this effect by cotransfection of EZH2 and ADRB2. As expected, EZH2 overexpression dramatically (12.9-fold, $p < 0.001$) increased invasion in H16N2 cells. By contrast, overexpression of ADRB2 led to a significant (3.6-fold, $p < 0.001$) reduction in EZH2-induced cell invasion (Figure 4D).

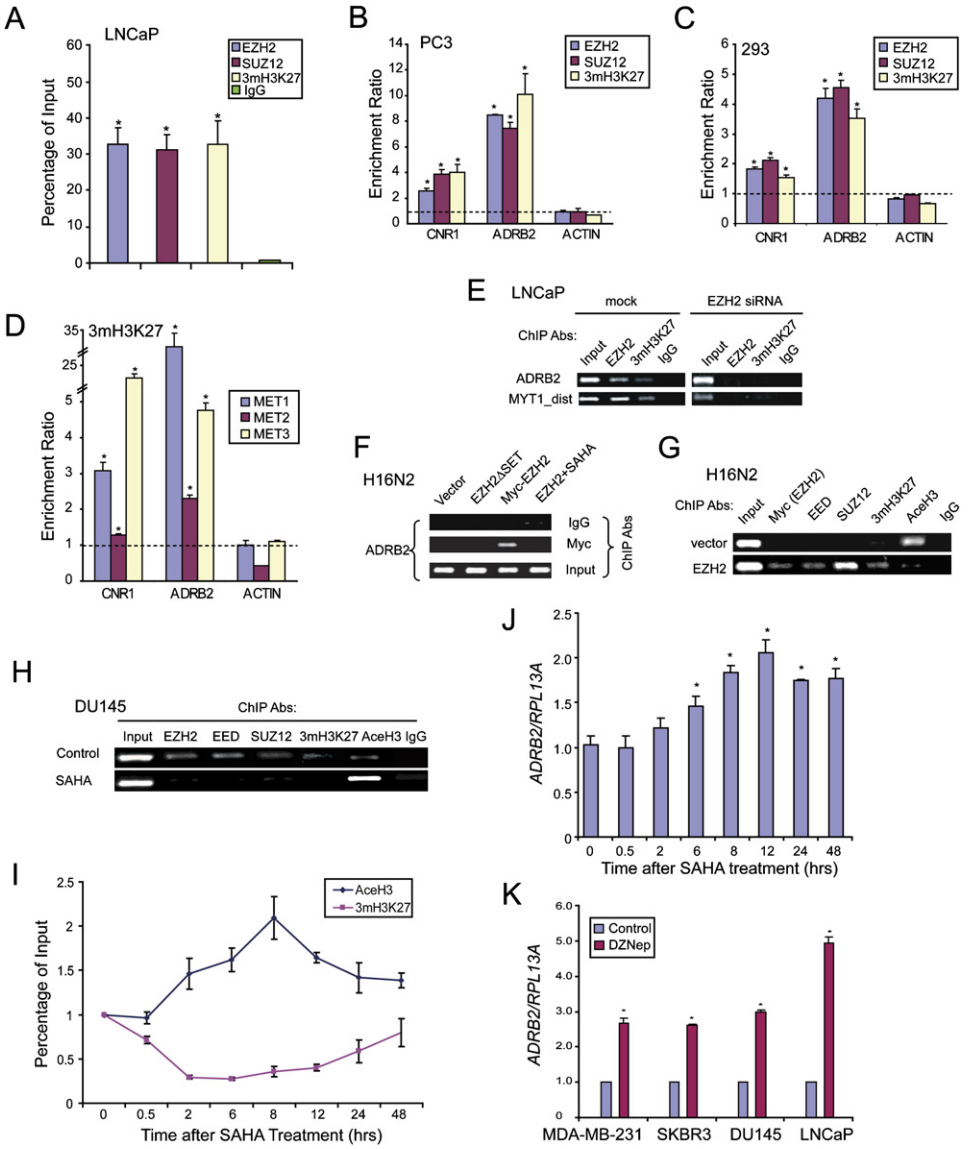

Figure 3. The *ADRB2* Promoter Is Occupied by PRC2 Complex Proteins and the H3K27 Trimethylation Mark

(A) Conventional ChIP-PCR analysis of EZH2 and SUZ12 occupancy and the level of H3K27 trimethylation (3mH3K27) of the *ADRB2* promoter. Chromatin immunoprecipitation (ChIP) were performed in LNCaP cells using antibodies against EZH2, SUZ12, 3mH3K27, and a control IgG. *ADRB2* promoter DNA was determined by PCR using primers specific to the *ADRB2* promoter (Table S3), as percentage of whole-cell extract (WCE) input DNA. Significance was calculated between antibody-enriched and IgG-enriched chromatin.

(B–D) EZH2, SUZ12, and 3mH3K27 occupancy on the *ADRB2* promoter in PC3 metastatic prostate cancer cell line (B), in 293 embryonic kidney cell line (C), and in three metastatic prostate cancer tissues (MET1-3) (D). ChIP-enriched chromatin was amplified by ligation-mediated PCR (LM-PCR) along with the WCE DNA. An equal amount (100 ng) of ChIP-enriched and input amplicons was used to test target promoters by gene-specific primers. The enrichment of a target promoter was assessed as the enrichment ratio of ChIP-enriched to WCE amplicons. *CNR1* is a positive control gene (Kirmizis et al., 2004), and *ACTIN* is a negative control. The dashed line indicates no enrichment. Significant enrichment of target genes was assessed relative to *ACTIN*.

(E) EZH2 RNA interference blocks EZH2 and 3mH3K27 binding to the *ADRB2* promoter. *MYT1*_distal is a positive control gene known to interact with PRC2 complex (Kirmizis et al., 2004). ChIP experiments were performed using antibodies in LNCaP cells that were incubated with EZH2 siRNA or no siRNA (mock) control. For the siRNA transfections, cells were treated with siRNA duplex for 72 hr, then replated and incubated with fresh siRNA duplex for another 72 hr.

(F) Ectopically expressed EZH2 binds *ADRB2* promoter in a histone deacetylation-dependent manner. ChIP was performed in H16N2 cells infected with vector, EZH2ΔSET, or EZH2 adenovirus alone or in combination with SAHA treatment and analyzed by PCR using gene-specific primers. An anti-Myc antibody was used for ChIP to specifically detect ectopically expressed EZH2 and its mutants.

(G) Ectopic overexpression of EZH2 increases PRC2 complex occupancy and H3K27 trimethylation and reduces H3 acetylation at the *ADRB2* promoter. H16N2 cells infected by vector or EZH2 adenovirus were subjected to ChIP using the antibodies listed.

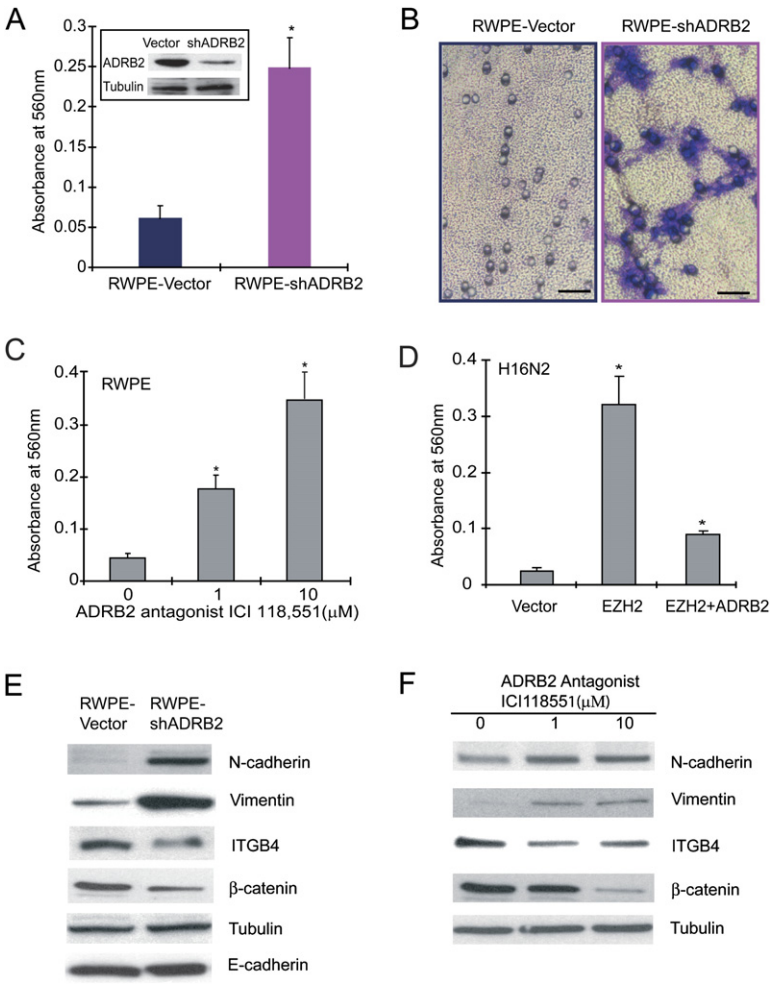

Figure 4. ADRB2 Inhibition Confers Cell Invasion and Transforms Benign Prostate Epithelial Cells

(A and B) RWPE-shADRB2 cells were assayed for invasion through a modified basement membrane chamber assay. (Inset) Immunoblot analysis of ADRB2 protein in stable vector and RWPE-shADRB2 cell lines. The benign immortalized prostate cell line RWPE was transfected with shRNA constructs targeting ADRB2 or control vector, and stable RWPE-shADRB2 or vector clones were generated. Scale bar, 100 μm.

(C) ADRB2 inactivation by antagonist in noninvasive benign RWPE epithelial cells leads to increased invasion. The noninvasive RWPE cells were treated with 0, 1, or 10 μM of an ADRB2-specific antagonist ICI 118,551 and assessed by invasion assay.

(D) ADRB2 activation interferes with EZH2-mediated cell invasion. H16N2 cells were infected with vector or EZH2 alone or in combination with ADRB2. In this panel, the significance of invasion in cells treated with EZH2 only was evaluated relative to vector control, whereas cells treated by EZH2 in combination with ADRB2 were evaluated relative to the EZH2-treated cells.

(E and F) ADRB2 inhibition in RWPE benign prostate epithelial cells, either by shRNA targeting ADRB2 (RWPE-shADRB2) (E) or by an ADRB2 antagonist ICI 118,551 (F), regulates the expression of EMT biomarkers and cell adhesion molecules.

Error bars: n = 3, mean ± SEM, *p < 0.001.

We examined the stable RWPE-shADRB2 cells for other malignant phenotypes besides cell invasion and migration. Interestingly, we observed that the RWPE-shADRB2 cells display a mesenchymal phenotype with fibroblast-like shape, whereas the vector control cells appear more rounded (Figure S7). Importantly, this morphological conversion highly resembles the converse of the mesenchymal-to-epithelial transition by constitutively active Rap1A, a primary downstream effector of β-adrenergic signaling (Price et al., 2004). To confirm that ADRB2 inhibition in fact transformed the RWPE benign prostate epithelial cells, we examined the expression of typical mesenchymal biomarkers and adhesion molecules. Immunoblot analysis demonstrated markedly increased expression of the mesenchymal cell biomarkers vimentin and N-cadherin, and yet a significant decrease of the expression of adhesion molecules β-catenin and integrin β 4 (ITGB4) (Figure 4E). No significant changes in E-cadherin expression were observed. Interestingly, antagonist (ICI 118,551)-mediated inactivation of ADRB2 recaptured the expressional changes in RWPE-shADRB2 cells (Figure 4F). Furthermore, to investigate whether this property of ADRB2 has a link to EZH2 function, we overexpressed EZH2 in native RWPE cells. Interestingly, EZH2 overexpression evoked expressional

(H) Endogenous PRC2 complex occupies the *ADRB2* promoter and is sensitive to the HDAC inhibitor SAHA. ChIP experiments were performed in DU145 cells following control or SAHA treatment using the antibodies listed.

For (E)–(H), PCR was performed using antibody-enriched chromatin without LM-PCR amplification. Enrichment of target gene by a ChIP antibody is assessed relative to the IgG control.

(I) PRC2 recruitment to the *ADRB2* promoter after a time course of SAHA treatment. DU145 prostate cancer cells were treated with 1 μM SAHA and harvested at 0, 0.5, 2, 6, 8, 12, 24, and 48 hr after treatment. ChIP was performed using antibodies against AceH3 and 3mH3K27. Standard qPCR was done using primers for *ADRB2* promoter, and ChIP enrichment was evaluated as a percentage of input DNA.

(J) *ADRB2* transcript was upregulated following SAHA treatment. QRT-PCR analysis of *ADRB2* transcripts was done following a time course of SAHA treatment. *RPL13A* was used for normalization as it was reported to be insensitive to HDAC inhibitors (Mogal and Abdulkadir, 2006).

(K) Marked upregulation of *ADRB2* transcript by the PRC2-inhibiting compound DZNep. Cells were treated with 5 μM DZNep for 48 hr and were harvested for RNA isolation and QRT-PCR analysis.

Error bars: n = 3, mean ± SEM, *p < 0.01 by Student's t test.

changes analogous to the inhibition of ADRB2. Remarkably, reactivation of ADRB2 in the EZH2-overexpressing RWPE cells is able to reverse the effect induced by EZH2 overexpression (data not shown).

ADRB2 Inhibits Prostate Tumor Growth In Vivo

We have thus far established a role for β-adrenergic signaling in cell migration, invasion, and transformation by using in vitro cell line models. It is appealing to extend this study to in vivo mouse models. We first tested the effect of stable EZH2 knockdown, leading to consequent ADRB2 induction (Figure 2E), on prostate tumor formation by inoculating the EZH2−/ADRB2+ DU145-shEZH2 cells into nude mice. Intriguingly, tumors developed in all control EZH2+/ADRB2− mice at 3 weeks after injection, whereas the EZH2−/ADRB2+ mice did not grow tumors by 7 weeks after injection (Figure 5A).

To directly examine the effect of ADRB2 in in vivo prostate tumor growth, we subcutaneously injected native DU145 prostate cancer cells into nude mice. These mice were then randomly separated into three groups (five mice per group) and treated, through intraperitoneal injections, with either PBS or the ADRB2 agonist isoproterenol at 400 μg/day or 800 μg/day. Xenograft tumors started to grow at 2 weeks after implantation. When compared with the PBS-treated control group, isoproterenol-treated mice developed significantly (two-sample Student's t test, $p = 0.006$) smaller tumors (Figure 5B).

ADRB2 Protein Level Predicts Prostate Cancer Clinical Outcome

The repression of ADRB2 by oncogenic EZH2 and its implication in cell invasion and tumorigenesis in both in vitro and in vivo models suggest that reduced expression of ADRB2 may be associated with human prostate cancer progression. To assess *ADRB2* expression during human prostate cancer progression, we examined a prostate cancer microarray study (Varambally et al., 2005) that profiled six benign prostate tissue samples, seven clinically localized prostate cancers, and six metastatic prostate cancers. We found that *ADRB2* transcript is strongly repressed ($p = 0.003$ by Student's t test) in the metastatic samples, being inversely associated ($r = -0.85$, $p < 0.0001$) with *EZH2* expression (Figure 5C). It is possible that ADRB2 may present in the stromal cells and its downregulation in metastatic prostate cancer merely reflects the decrease in the percentage of stroma. To exclude this possibility, we examined *ADRB2* expression in a prostate cancer microarray profiling data set using laser capture microdissected (LCM) epithelial cells (Tomlins et al., 2007). Importantly, cDNA microarray analysis of 30 LCM PCA and 16 MET samples confirmed downregulation ($p < 0.001$ by Student's t test) of *ADRB2* in metastatic prostate cancer (Figure 5D).

To evaluate ADRB2 protein expression in prostate tumors, ADRB2 immunohistochemistry was performed in 36 benign, 6 prostatic intraepithelial neoplasia (PIN), 82 clinically localized PCA, and 16 MET tissues. As expected, we observed ADRB2 staining primarily in epithelial cells (Figure 5E). Overall, there was a significant difference in the distribution of median ADRB2 staining intensity among the four groups ($p < 0.0001$ by Kruskal-Wallis test). Notably, the metastatic tumors had the weakest expression of ADRB2. Most cases of low or absent ADRB2 staining were observed in METs (Figures 5E and F). This led us to the hypothesis that *low* ADRB2 protein levels may portend the aggressiveness of clinically localized prostate cancer. This would be in contrast to *high* EZH2 levels being indicative of poor clinical outcome in patients with clinically localized disease (Varambally et al., 2002).

We therefore examined the clinical outcome of the 82 patients with organ-confined prostate cancer, taking into account clinical and pathological parameters. By Kaplan-Meier analysis, a low product score (<240) indicative of low ADRB2 staining was significantly ($p = 0.002$) associated with clinical failure, in comparison with high product score (≥240) indicative of strong ADRB2 staining (Figure 5G). Multivariate Cox proportional-hazards regression analysis revealed that ADRB2 could predict clinical failure independently of Gleason score, maximum tumor dimension, surgical margin status, and preoperative PSA (Table 1). With an overall recurrence ratio of 3.4 (95% CI: 1.5–7.8, $p = 0.004$), it was by far the strongest predictor of clinical failure in this model. In order to compare the ability of ADRB2 status to predict outcomes beyond that given with standard clinical parameters, we compared ADRB2 with a preoperative nomogram for predicting treatment failure at 5 years (Kattan et al., 1998). As shown in Table 2, ADRB2 provides significant predictive power for patient prognosis ($p = 0.015$, recurrence ratio = 2.7, 95% CI: 1.2–6.0) that is both independent of the preoperative nomogram and of greater significance. Taken together, ADRB2 is downregulated in metastatic prostate cancer, low ADRB2 expression is associated with poor prognosis of clinically localized prostate cancer, and ADRB2 expression provides additional prognostic information beyond a typical clinical nomogram.

DISCUSSION

EZH2 is a transcriptional repressor that has been found upregulated in a number of cancer types (Bachmann et al., 2006; Collett et al., 2006; Varambally et al., 2002). Dysregulation of EZH2 controls cell proliferation, cell invasion, and transformation (Bracken et al., 2003; Croonquist and Van Ness, 2005). However, it remains unknown how EZH2 overexpression leads to cancer initiation and progression. One mechanism is that the transcriptional repressor EZH2 may promote tumorigenesis by the repression of tumor suppressor genes (Beke et al., 2007). Identifying direct EZH2 target genes with potential tumor suppressor function may reveal novel prognostic/diagnostic biomarkers and therapeutic targets. Thus, in this study we nominate and evaluate potential targets of EZH2 and characterize one of these target genes, ADRB2, in prostate cancer progression. In order to increase our chance of identifying truly positive target genes, we have integrated multiple diverse genomic data, as each of these data sets may have false

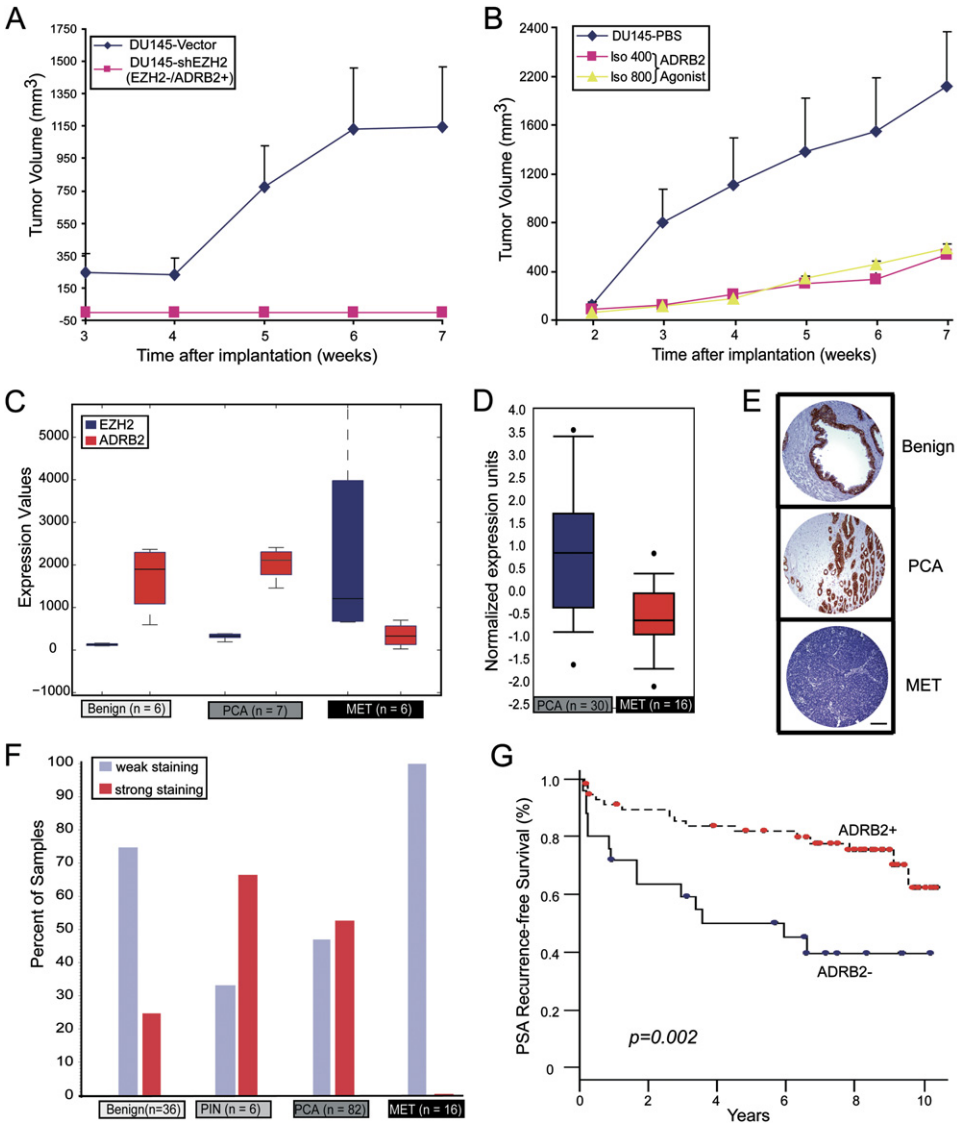

Figure 5. ADRB2 Expression Correlates with Prostate Cancer Progression

(A) The stable DU145-shEZH2 (EZH2−/ADRB2+) cells have inhibited tumor growth in a xenograft mouse model. Mice were divided into two groups (n = 5) and inoculated with control or EZH2−/ADRB2+ DU145 cells (Figure 2E). Tumor sizes were evaluated once per week. All control mice formed tumors by 2 weeks postinoculation, where as no tumors formed by the EZH2−/ADRB2+ cells at 7 weeks postinoculation. Error bars: n = 5, mean ± SEM.

(B) ADRB2 activation inhibits tumor growth in a xenograft mouse model. Mice were injected with DU145 cells, were randomly divided into three groups (n = 5 per group), and received intraperitoneal injection of either PBS or the ADRB2 agonist Isoproterenol (at 400 μg/day or 800 μg/day) once per day. Tumor sizes were evaluated once per week. Isoproterenol treatment significantly (two-sample Student's t test, p = 0.006) inhibited xenograft tumor growth. Error bars: n = 5, mean ± SEM.

(C) Affymetrix microarray analysis of grossly dissected tissues including six benign, seven clinically localized (PCA), and six metastatic prostate cancer (METs) tissues. Box plot of ADRB2 (red) and EZH2 (blue) expression in each category is shown.

(D) cDNA microarray analysis of laser capture microdissected (LCM) prostate cancer epithelial cells for ADRB2 expression. Box plot of ADRB2 expression in a cohort of 30 LCM localized prostate cancer (PCA, in blue) and 16 metastatic prostate cancer (MET, in red) tissues is shown.

(E) Representative immunostaining of ADRB2 in benign prostate and localized (PCA) and metastatic (MET) prostate cancer. Scale bar, 100 μm.

(F) Histogram of ADRB2 immunostaining as assessed using prostate cancer tissue microarray analysis (TMA). Samples were scored (range: 1, 2, 3, and 4) based on median staining intensity. A score of 4 and higher is considered as strong staining, while scores of 3 and less are considered weak staining. PIN stands for *p*rostate *i*ntraepithelial *n*eoplasia.

(G) Kaplan-Meier analysis shows that individuals with clinically localized PCA that have lower expression of ADRB2 (low intensity and low percentage of staining) have a greater risk for disease recurrence after prostatectomy (p = 0.002).

Table 1. Multivariate Cox Regression Analysis of Association of ADRB2 and Clinical Parameters with Cancer Recurrence

	Recurrence Ratio	95% CI		p
ADRB2 (product score ≥ 240 versus < 240)	3.423	1.500	7.808	0.004
Gleason (≥7 versus ≤6)	1.604	0.607	4.241	0.341
Tumor size (≥2 cm versus <2 cm)	1.306	0.526	3.239	0.565
Surgical margin (positive versus negative)	1.737	0.807	3.740	0.158
Preoperative PSA (>7, 4–7, ≤4)	1.519	0.852	2.707	0.156

Note: Sample size is 82 with 29 recurrences. Product score indicates the product of ADRB2 intensity measure (range: 1, 2, 3, and 4) and percentage of staining measure (range: 0–100).

positives. In addition, as noted by Squazzo et al. (2006) with regards to the cell type specificity of PcG target genes, the targets identified in this study, which is oriented specifically toward prostate and breast cancer cells, may not be universal to other cell types. As EZH2 functions as a transcriptional repressor, it may have profound effects on target gene regulation; it is possible that multiple downstream effectors of EZH2 exist and may likewise mediate EZH2 function as redundant pathways. However, our study suggests that ADRB2 is one of these targets with clinical relevance.

We provide multiple lines of evidence to support *ADRB2* as a target of EZH2-mediated transcriptional repression. First, our analysis revealed an inverse association between EZH2 and ADRB2 expression across multiple microarray tumor profiling data sets. By qPCR we confirmed this across a cohort of benign and prostate cancer samples. To exclude the possibility that ADRB2 downregulation in metastatic prostate cancer could be a bias of stromal cells, we examined microarray data using LCM tumor samples. Second, we have experimentally altered EZH2 expression in vitro across multiple prostate and breast cell lines and investigated the corresponding changes in ADRB2 expression. Multiple techniques, including adenovirus overexpression, siRNA-mediated transient inhibition, and shRNA-mediated stable inhibition, were used. Additionally, we have examined expression changes at both the transcript and protein levels. We have also performed immunofluorescent costaining of ADRB2 and EZH2 in vitro and tissue microarray staining of ADRB2 to examine expression changes at the cellular level. Taken together, our results provide compelling evidence that ADRB2 is a target for repression by EZH2 and that it is upregulated in metastatic prostate cancer.

By ChIP assay, we showed that the *ADRB2* promoter is occupied by the EZH2-containing PRC2 complex proteins and trimethylated at H3K27 across multiple cell lines as well as metastatic prostate cancer specimens. These results support the interaction between the EZH2 protein and the *ADRB2* promoter, thus providing a mechanism for the repression of ADRB2 by EZH2. Furthermore, we demonstrated that ectopically expressed EZH2 recruits other PRC2 complex proteins to the *ADRB2* promoter and the occupancy of the *ADRB2* promoter by the PRC2 complex can be removed by RNA interference of EZH2. Importantly, we observed that ADRB2 expression can be derepressed by PRC2-inhibiting compounds. These are consistent with the observed changes in ADRB2 expression following EZH2 overexpression or inhibition.

The EZH2-mediated repression of ADRB2 and its downregulation in metastatic prostate cancer suggest a role of ADRB2 in tumor suppression. ADRB2 is a member of the seven-transmembrane receptors, which are often referred to as GPCRs. Ligand binding on ADRB2 strongly increases its affinity with G protein and elevates the level of intracellular cAMP, which regulates a wide range of cellular processes by multiple mechanisms (Daaka, 2004; de Rooij et al., 1998). Stimulation of ADRB2 has been previously implicated in cell proliferation (Stork and Schmitt, 2002) and cell adhesion (Bos, 2005; Price et al., 2004). A hallmark of cAMP/β-adrenergic signaling is its ability to inhibit cell proliferation in some cell types while stimulating cell growth in others (Stork and Schmitt, 2002). In this study, however, we did not observe an effect of ADRB2 on cell proliferation in prostate cells. We observed, instead, that ADRB2 inhibition markedly increased invasiveness of benign prostate epithelial cells and immortalized normal breast epithelial cells, partially counteracting EZH2-mediated cell invasion.

Table 2. Multivariate Cox Regression Analysis of Association of ADRB2 and Preoperative Nomogram with Cancer Recurrence

	Recurrence Ratio	95% CI		p
ADRB2 (product score ≥ 240 versus < 240)	2.694	1.212	5.989	0.015
Preoperative nomogram for 5 year recurrence-free prediction	1.019	1.003	1.036	0.020
Tumor size (≥2 cm versus <2 cm)	1.146	0.470	2.791	0.764
Surgical margin (positive versus negative)	1.612	0.736	3.531	0.233
Age	1.009	0.960	1.061	0.716

Moreover, ADRB2 knockdown transformed the RWPE benign prostate epithelial cells, leading to changes in cell morphology and gene expression that are typical for epithelial-to-mesenchymal transition (EMT). Although ADRB2 has long been implicated in cell adhesion, our report demonstrates its additional roles in cell invasion and EMT. These results are consistent with the repression of ADRB2 by oncogenic EZH2 and the downregulation of ADRB2 in aggressive prostate tumors. Our xenograft mouse models suggest that ADRB2-activating compounds may have potential utility in treating prostate cancer in patients.

Importantly, by immunohistochemistry we found much lower or absent ADRB2 staining in metastatic prostate cancer relative to clinically localized tumors and benign prostate specimens. Significantly, analysis of ADRB2 staining in 82 localized prostate cancers with 29 cancer recurrence correlates ADRB2 expression with prostate cancer prognosis. The ADRB2 status provides additional predictive power beyond that achieved with standard preoperative nomograms. *Low* ADRB2 expression is significantly associated with PSA recurrence, thus indicating ADRB2 as a potential prognostic biomarker of aggressive prostate cancer. Therefore, we show that characterization of EZH2 direct target genes may be useful for the identification of novel cancer biomarkers and potential therapeutic targets.

In summary, we integrated multiple genomics data to identify ADRB2 as a direct target of EZH2-mediated transcriptional repression. We determined a role of ADRB2 in regulating cell invasion and tumorigenesis, thus providing a PcG target relevant to EZH2's oncogenic function and suggesting a functional link between PcG silencing and β-adrenergic signaling. In human prostate cancer, ADRB2 levels can be used as a prognostic biomarker and possibly to identify patients with aggressive disease (i.e., those with low levels of ADRB2). Further studies in the context of larger prospectively gathered cohorts will allow investigators to evaluate ADRB2 as a prognostic biomarker in different populations. Taken together, we demonstrate the power of integrating multiple diverse genomics data to decipher critical targets of disease-related genes.

EXPERIMENTAL PROCEDURES

Cell Culture

LNCaP and DU145 prostate cancer cells were cultured in RPMI supplemented with 10% fetal bovine serum (Invitrogen, Carlsband, CA). RWPE cells were grown in keratinocyte serum-free medium (Invitrogen) supplemented with 5 ng/ml human recombinant EGF and 0.05 mg/ml bovine pituitary extract. H16N2 immortalized human mammary epithelial cells were grown in Ham's F12 with supplements. Detailed information as well as treatment to cells is described in the Supplemental Experimental Procedures.

Human Tissue Specimens

Prostate cancer tissues were collected from the Rapid Autopsy Program, which is part of the University of Michigan Prostate Cancer Specialized Program of Research Excellence (S.P.O.R.E.) Tissue Core. Tissue samples were collected with informed consent of the patients and prior Institutional Review Board approval.

Tissue Microarray Analysis

The clinically stratified prostate cancer tissue microarrays used in this study have been described previously (Varambally et al., 2002). TMA of ADRB2 expression in prostate cancer was performed according to established protocols (Varambally et al., 2005). For Kaplan-Meier analysis, clinical failure was defined as either an increase of 0.2 ng ml^{-1} PSA or recurrence of disease after prostatectomy, such as development of metastatic cancer. ADRB2 protein level in each sample was measured based on its product score, which is a product of ADRB2 staining intensity measure at the levels of 1, 2, 3, and 4, and the percentage of positive staining measure ranged from 0% to 100%.

Gene Expression Analysis

Total RNA was isolated at various times after EZH2 infection (RWPE 3, 6, 12, 24, 48, 72 hr; H16N2 6, 12, 24, 48, 72 hr), or at 48 hr after EZH2 RNA interference in both cell lines. Gene expression analysis was done as described using 20k-element cDNA microarrays covering 15,495 UniGene clusters (Dhanasekaran et al., 2005). The hybridized slides were scanned by Axon scanner (Axon Instruments Inc., Union City, CA), the images were analyzed using Genepix, and data were analyzed as described in detail in the Supplemental Experimental Procedures. Gene expression microarray data discussed in this study have been deposited in the NCBI's Gene Expression Omnibus (GEO) with accession number GSE8144 and GSE8145.

ChIP and Genome-wide Location Analysis

ChIP was performed according to published protocols (Boyd et al., 1998). Genome-wide location analysis was performed per manufacturer's instruction (Aviva Systems Biology, San Diego, CA). Modifications and experimental details are indicated in the Supplemental Experimental Procedures. Primer sequences used for ChIP are listed in Table S3. Genome-wide location data discussed in this study have been deposited in the NCBI's Gene Expression Omnibus (GEO) with accession number GSE5596.

Murine Prostate Tumor Xenograft Model

All procedures involving mice were approved by the University Committee on Use and Care of Animals (UCUCA) at the University of Michigan and conform to their relevant regulatory standards. Five-week-old male nude athymic BALB/c nu/nu mice (Charles River Laboratory, Wilmington, MA) were used for examining the tumorigenicity. To evaluate the role of EZH2 downregulation in tumor formation, the EZH2−/ADRB2+ DU145 cells or the vector control cells were propagated and inoculated by subcutaneous injection into the dorsal flank of ten mice (n = 5 per group). To evaluate the role of β-adrenergic signaling in tumor formation, DU145 cell was propagated and treated with PBS or 10 μM Isoproterenol at 24 hr prior to harvest. Cells were then harvested and suspended in a 0.1 ml PBS with or without treatment of 10 μM Isoproterenol. A total of 15 mice (n = 5 per group) were each implanted with 5×10^6 DU145 cells into the dorsal flank subcutaneously. Treatment started 24 hr after implantation. Each group was administered daily by intraperitoneal injection with either PBS or Isoproterenol (at 400 μg/day or 800 μg/day). Tumor size was measured every week, and tumor volumes were estimated using the formula $(\pi/6)$ $(L \times W^2)$, where L = length of tumor and W = width.

Supplemental Data

The Supplemental Data include supplemental text, seven supplemental figures, and three supplemental tables and can be found with this article online at http://www.cancercell.org/cgi/content/full/12/5/419/DC1/.

ACKNOWLEDGMENTS

The authors would like to thank Xiaoju Wang for helpful discussions, Wenjun Zhou for technical assistance, and the staff of the Microscopy and Image Analyses laboratory at the University of Michigan for their help in cell imaging. A.M.C. is supported by a Burroughs Welcome

Foundation Award in Clinical Translational Research. S.A.T. is supported by the Medical Scientist Training Program and a Rackham Pre-doctoral Award. This research was supported in part by National Institutes of Health Grant RO1 CA97063 (to A.M.C. and D.G.); U01 CA111275 (to A.M.C. and D.G.); P50 CA69568 (to A.M.C. and D.G.); and Department of Defense Grants PC040517 (to R.M.), PC051081 (to A.M.C. and S.V.), and PC060266 (to J.Y.). For V.E.M., this research was supported in part by the intramural research program of the NIH, Center for Cancer Research, NCI-Frederick. The Oncomine database was used initially in this manuscript. Oncomine is freely available to the academic community. Commercial rights to Oncomine have been licensed to Compendia Biosciences. A.M.C. is a cofounder of Compendia Biosciences and serves as head of the scientific advisory board.

Received: June 8, 2007
Revised: August 22, 2007
Accepted: October 9, 2007
Published: November 12, 2007

REFERENCES

Bachmann, I.M., Halvorsen, O.J., Collett, K., Stefansson, I.M., Straume, O., Haukaas, S.A., Salvesen, H.B., Otte, A.P., and Akslen, L.A. (2006). EZH2 expression is associated with high proliferation rate and aggressive tumor subgroups in cutaneous melanoma and cancers of the endometrium, prostate, and breast. J. Clin. Oncol. *24*, 268–273.

Beke, L., Nuytten, M., Van Eynde, A., Beullens, M., and Bollen, M. (2007). The gene encoding the prostatic tumor suppressor PSP94 is a target for repression by the Polycomb group protein EZH2. Oncogene *26*, 4590–4595.

Bos, J.L. (2005). Linking Rap to cell adhesion. Curr. Opin. Cell Biol. *17*, 123–128.

Boyd, K.E., Wells, J., Gutman, J., Bartley, S.M., and Farnham, P.J. (1998). c-Myc target gene specificity is determined by a post-DNA binding mechanism. Proc. Natl. Acad. Sci. USA *95*, 13887–13892.

Boyer, L.A., Plath, K., Zeitlinger, J., Brambrink, T., Medeiros, L.A., Lee, T.I., Levine, S.S., Wernig, M., Tajonar, A., Ray, M.K., et al. (2006). Polycomb complexes repress developmental regulators in murine embryonic stem cells. Nature *441*, 349–353.

Bracken, A.P., Pasini, D., Capra, M., Prosperini, E., Colli, E., and Helin, K. (2003). EZH2 is downstream of the pRB-E2F pathway, essential for proliferation and amplified in cancer. EMBO J. *22*, 5323–5335.

Bracken, A.P., Dietrich, N., Pasini, D., Hansen, K.H., and Helin, K. (2006). Genome-wide mapping of Polycomb target genes unravels their roles in cell fate transitions. Genes Dev. *20*, 1123–1136.

Cao, R., Wang, L., Wang, H., Xia, L., Erdjument-Bromage, H., Tempst, P., Jones, R.S., and Zhang, Y. (2002). Role of histone H3 lysine 27 methylation in Polycomb-group silencing. Science *298*, 1039–1043.

Collett, K., Eide, G.E., Arnes, J., Stefansson, I.M., Eide, J., Braaten, A., Aas, T., Otte, A.P., and Akslen, L.A. (2006). Expression of enhancer of zeste homologue 2 is significantly associated with increased tumor cell proliferation and is a marker of aggressive breast cancer. Clin. Cancer Res. *12*, 1168–1174.

Croonquist, P.A., and Van Ness, B. (2005). The polycomb group protein enhancer of zeste homolog 2 (EZH 2) is an oncogene that influences myeloma cell growth and the mutant ras phenotype. Oncogene *24*, 6269–6280.

Daaka, Y. (2004). G proteins in cancer: The prostate cancer paradigm. Sci. STKE *2004*, re2.

de Rooij, J., Zwartkruis, F.J., Verheijen, M.H., Cool, R.H., Nijman, S.M., Wittinghofer, A., and Bos, J.L. (1998). Epac is a Rap1 guanine-nucleotide-exchange factor directly activated by cyclic AMP. Nature *396*, 474–477.

Dhanasekaran, S.M., Dash, A., Yu, J., Maine, I.P., Laxman, B., Tomlins, S.A., Creighton, C.J., Menon, A., Rubin, M.A., and Chinnaiyan, A.M. (2005). Molecular profiling of human prostate tissues: Insights into gene expression patterns of prostate development during puberty. FASEB J. *19*, 243–245.

Glinsky, G.V., Glinskii, A.B., Stephenson, A.J., Hoffman, R.M., and Gerald, W.L. (2004). Gene expression profiling predicts clinical outcome of prostate cancer. J. Clin. Invest. *113*, 913–923.

Huang, E., Cheng, S.H., Dressman, H., Pittman, J., Tsou, M.H., Horng, C.F., Bild, A., Iversen, E.S., Liao, M., Chen, C.M., et al. (2003). Gene expression predictors of breast cancer outcomes. Lancet *361*, 1590–1596.

Kattan, M.W., Eastham, J.A., Stapleton, A.M., Wheeler, T.M., and Scardino, P.T. (1998). A preoperative nomogram for disease recurrence following radical prostatectomy for prostate cancer. J. Natl. Cancer Inst. *90*, 766–771.

Kirmizis, A., Bartley, S.M., Kuzmichev, A., Margueron, R., Reinberg, D., Green, R., and Farnham, P.J. (2004). Silencing of human polycomb target genes is associated with methylation of histone H3 Lys 27. Genes Dev. *18*, 1592–1605.

Kleer, C.G., Cao, Q., Varambally, S., Shen, R., Ota, I., Tomlins, S.A., Ghosh, D., Sewalt, R.G., Otte, A.P., Hayes, D.F., et al. (2003). EZH2 is a marker of aggressive breast cancer and promotes neoplastic transformation of breast epithelial cells. Proc. Natl. Acad. Sci. USA *100*, 11606–11611.

Kuzmichev, A., Nishioka, K., Erdjument-Bromage, H., Tempst, P., and Reinberg, D. (2002). Histone methyltransferase activity associated with a human multiprotein complex containing the Enhancer of Zeste protein. Genes Dev. *16*, 2893–2905.

Lamb, J., Ramaswamy, S., Ford, H.L., Contreras, B., Martinez, R.V., Kittrell, F.S., Zahnow, C.A., Patterson, N., Golub, T.R., and Ewen, M.E. (2003). A mechanism of cyclin D1 action encoded in the patterns of gene expression in human cancer. Cell *114*, 323–334.

Lee, T.I., Jenner, R.G., Boyer, L.A., Guenther, M.G., Levine, S.S., Kumar, R.M., Chevalier, B., Johnstone, S.E., Cole, M.F., Isono, K., et al. (2006). Control of developmental regulators by Polycomb in human embryonic stem cells. Cell *125*, 301–313.

Levine, S.S., Weiss, A., Erdjument-Bromage, H., Shao, Z., Tempst, P., and Kingston, R.E. (2002). The core of the polycomb repressive complex is compositionally and functionally conserved in flies and humans. Mol. Cell. Biol. *22*, 6070–6078.

Matsukawa, Y., Semba, S., Kato, H., Ito, A., Yanagihara, K., and Yokozaki, H. (2006). Expression of the enhancer of zeste homolog 2 is correlated with poor prognosis in human gastric cancer. Cancer Sci. *97*, 484–491.

Mogal, A., and Abdulkadir, S.A. (2006). Effects of Histone Deacetylase Inhibitor (HDACi); Trichostatin-A (TSA) on the expression of housekeeping genes. Mol. Cell. Probes *20*, 81–86.

Price, L.S., Hajdo-Milasinovic, A., Zhao, J., Zwartkruis, F.J., Collard, J.G., and Bos, J.L. (2004). Rap1 regulates E-cadherin-mediated cell-cell adhesion. J. Biol. Chem. *279*, 35127–35132.

Raaphorst, F.M., Meijer, C.J., Fieret, E., Blokzijl, T., Mommers, E., Buerger, H., Packeisen, J., Sewalt, R.A., Otte, A.P., and van Diest, P.J. (2003). Poorly differentiated breast carcinoma is associated with increased expression of the human polycomb group EZH2 gene. Neoplasia *5*, 481–488.

Ramaswamy, S., Tamayo, P., Rifkin, R., Mukherjee, S., Yeang, C.H., Angelo, M., Ladd, C., Reich, M., Latulippe, E., Mesirov, J.P., et al. (2001). Multiclass cancer diagnosis using tumor gene expression signatures. Proc. Natl. Acad. Sci. USA *98*, 15149–15154.

Rastelli, L., Chan, C.S., and Pirrotta, V. (1993). Related chromosome binding sites for zeste, suppressors of zeste and Polycomb group proteins in Drosophila and their dependence on Enhancer of zeste function. EMBO J. *12*, 1513–1522.

Rhodes, D.R., Yu, J., Shanker, K., Deshpande, N., Varambally, R., Ghosh, D., Barrette, T., Pandey, A., and Chinnaiyan, A.M. (2004). ONCOMINE: A cancer microarray database and integrated data-mining platform. Neoplasia *6*, 1–6.

Ringrose, L., and Paro, R. (2004). Epigenetic regulation of cellular memory by the Polycomb and Trithorax group proteins. Annu. Rev. Genet. *38*, 413–443.

Squazzo, S.L., O'Geen, H., Komashko, V.M., Krig, S.R., Jin, V.X., Jang, S.W., Margueron, R., Reinberg, D., Green, R., and Farnham, P.J. (2006). Suz12 binds to silenced regions of the genome in a cell-type-specific manner. Genome Res. *16*, 890–900.

Stork, P.J., and Schmitt, J.M. (2002). Crosstalk between cAMP and MAP kinase signaling in the regulation of cell proliferation. Trends Cell Biol. *12*, 258–266.

Takezaki, T., Hamajima, N., Matsuo, K., Tanaka, R., Hirai, T., Kato, T., Ohashi, K., and Tajima, K. (2001). Association of polymorphisms in the beta-2 and beta-3 adrenoceptor genes with risk of colorectal cancer in Japanese. Int. J. Clin. Oncol. *6*, 117–122.

Tan, J., Yang, X., Zhuang, L., Jiang, X., Chen, W., Lee, P.L., Karuturi, R.K., Tan, P.B., Liu, E.T., and Yu, Q. (2007). Pharmacologic disruption of Polycomb-repressive complex 2-mediated gene repression selectively induces apoptosis in cancer cells. Genes Dev. *21*, 1050–1063.

Tomlins, S.A., Mehra, R., Rhodes, D.R., Cao, X., Wang, L., Dhanasekaran, S.M., Kalyana-Sundaram, S., Wei, J.T., Rubin, M.A., Pienta, K.J., et al. (2007). Integrative molecular concept modeling of prostate cancer progression. Nat. Genet. *39*, 41–51.

van 't Veer, L.J., Dai, H., van de Vijver, M.J., He, Y.D., Hart, A.A., Mao, M., Peterse, H.L., van der Kooy, K., Marton, M.J., Witteveen, A.T., et al. (2002). Gene expression profiling predicts clinical outcome of breast cancer. Nature *415*, 530–536.

Varambally, S., Dhanasekaran, S.M., Zhou, M., Barrette, T.R., Kumar-Sinha, C., Sanda, M.G., Ghosh, D., Pienta, K.J., Sewalt, R.G., Otte, A.P., et al. (2002). The polycomb group protein EZH2 is involved in progression of prostate cancer. Nature *419*, 624–629.

Varambally, S., Yu, J., Laxman, B., Rhodes, D.R., Mehra, R., Tomlins, S.A., Shah, R.B., Chandran, U., Monzon, F.A., Becich, M.J., et al. (2005). Integrative genomic and proteomic analysis of prostate cancer reveals signatures of metastatic progression. Cancer Cell *8*, 393–406.

Visser, H.P., Gunster, M.J., Kluin-Nelemans, H.C., Manders, E.M., Raaphorst, F.M., Meijer, C.J., Willemze, R., and Otte, A.P. (2001). The Polycomb group protein EZH2 is upregulated in proliferating, cultured human mantle cell lymphoma. Br. J. Haematol. *112*, 950–958.

Yu, Y.P., Landsittel, D., Jing, L., Nelson, J., Ren, B., Liu, L., McDonald, C., Thomas, R., Dhir, R., Finkelstein, S., et al. (2004). Gene expression alterations in prostate cancer predicting tumor aggression and preceding development of malignancy. J. Clin. Oncol. *22*, 2790–2799.

Accession Numbers

The data discussed in this publication have been deposited in NCBI's Gene Expression Omnibus (GEO; http://www.ncbi.nlm.nih.gov/geo/) and are accessible through GEO Series accession numbers GSE8144, GSE8145, and GSE5596.